Send Orders for Reprints to reprints@benthamscience.ae

Current Cancer Drug Targets, 2017, *17*, 1-13

RESEARCH ARTICLE

JQ1, a BET Inhibitor, Synergizes with Cisplatin and Induces Apoptosis in Highly Chemoresistant Malignant Pleural Mesothelioma Cells[#]

Ilaria Zanellato[a,*], Donato Colangelo[b] and Domenico Osella[a]

[a]*Dipartimento di Scienze ed Innovazione Tecnologica (DiSIT), Università del Piemonte Orientale, viale Teresa Michel 11, 15121 Alessandria, Italy;* [b]*Dipartimento di Scienze della Salute (DiSS), Università del Piemonte Orientale, via Solaroli 17, 28100 Novara, Italy*

Abstract: ***Background*:** Malignant pleural mesothelioma (MPM) is an asbestos-associated tumor with poor prognosis and few therapeutic options. JQ1, a selective antagonist of BRD4, modulates transcription of oncogenes, including MPM chemoresistance-associated c-Myc and Fra-1.

***Objective*:** We investigated if JQ1 could enhance the efficacy of cisplatin against MPM.

***Methods*:** The antiproliferative activity of cisplatin in combination with JQ1 was assessed on MPM cell lines representative of the cellular phenotypes of this tumor (epithelioid, sarcomatoid and biphasic), and on one cisplatin resistant sub-line. The combination schedule was optimized adopting a 3D-spheroid model. Drug combination effects were correlated with cell cycle distribution and senescence-associated β-galactosidase positive cells. The expression of c-Myc and Fra-1 proteins and some apoptosis markers was assessed by immunoblotting and RT-qPCR. DNA damage and repair were evaluated by means of alkaline comet assay.

***Results*:** JQ1 in combination with cisplatin elicited additive or synergistic (superadditive) antiproliferative effects on MPM cells, depending on the cell line. The combination showed tumor regression on the 3D-spheroid model. It induced increased apoptosis, along with decreased c-Myc and, sometimes, Fra-1 expression, JQ1 decreased cisplatin-induced DNA breaks in all MPM cells and increased senescence even in less proficient cells, thus enhancing the DNA damage response (DDR).

***Conclusion*:** The superadditive effect is due to c-Myc repression. The consequent DDR enhancement lead to apoptosis induction and/or permanent growth arrest (senescence), depending on the MPM cellular context, leading to tumor regression. Thus, the pharmacological modulation of BET activity could represent a promising tool for future MPM therapy.

ARTICLE HISTORY

Received: February 06, 2017
Revised: May 08, 2017
Accepted: June 05, 2017

DOI:
10.2174/1568009617666170623101722

Keywords: Malignant Mesothelioma, BET Bromodomain Inhibition, JQ1, Epigenetics, Platinum-based chemotherapy, c-Myc, Fra-1.

1. INTRODUCTION

Malignant pleural mesothelioma (MPM) is a tumor associated to occupational and environmental exposure to asbestos. Due to the long latency of MPM, estimated in 20-40 years, the reduction of asbestos contamination achieved in many countries, including Italy, will unlikely modify in the short period the risk of developing MPM and other asbestos-related diseases. Indeed, the incidence of this pathology, although relatively rare, is expected to show a maximum over the coming decade. MPM is a very aggressive form of cancer derived from the pleura mesothelium (80% of all mesotheliomas), pericardium and peritoneum. The majority of MPM patients are treated mainly to improve their quality of life, rather than prolong survival, since median life expectation after diagnosis ranges from 9-17 months. The actual approach to MPM treatment is multimodal (trimodal therapy) *i.e.* the combination of surgery, adjuvant or neoadjuvant chemotherapy, and radiation [1].

The current standard first-line treatment for advanced and unresectable MPM is cisplatin (or carboplatin) and antifolate-based (pemetrexed or raltitrexed) combination therapy. Several target-specific approaches have been explored, with limited results [2].

MPM is a tumor highly resistant to any drug. The prolonged exposure of mesothelium to asbestos likely induces high levels of ROS, either from the mineral itself and from the inclusive macrophages while trying to clear the tissue from the fibers. This prolonged inflammation leads to the selection of mutated cells characterized by high antioxidant, DNA-repair, and antiapoptotic armory, while the apoptotic pathways are mainly down-regulated [3, 4]. Accordingly, our *in vitro* MPM cell panel, composed of three cell lines representative of the different histotypes BR95 (epithelioid), MG06 (mixed), MM98 (sarcomatoid) cell line, and a cisplatin–resistant sub-line, MM98R, has previously shown marked chemoresistance [5]. In particular, the epithelioid

*Address correspondence to this author at the Dipartimento di Scienze ed Innovazione Tecnologica (DiSIT), Università del Piemonte Orientale, P.O. Box: 15121, Alessandria, Italy; Tel: +39-0131-360268; Fax: +39-0131-360250; E-mail: ilaria.zanellato@uniupo.it

[#]*Dedicated to the memory of Dr. Pier Giacomo Betta, the former coordinator of Mesothelioma Biobank, Alessandria National Hospital (Italy)*

1568-0096/17 $58.00+.00

cell line was highly resistant to any Pt-based drugs [6-9] and did not undergo apoptosis [10].

Cisplatin is the archetypal DNA-damaging metal-drug: it gives intra- and inter-strand DNA adducts that inhibit both transcription and replication. The most abundant intrastrand Pt-DNA lesions are tolerated via by-pass DNA polymerases or repaired by the nucleotide excision repair (NER) pathway. The lesion is excised, leaving two single strand breaks (SSB), and the resulting gap is refilled [11]. The basal NER machinery efficiently repairs lesions without activating the DNA damage response (DDR) [12]. DDR is a crucial signaling pathway, that in response to genetic insults, allows damage recognition, activation of cell cycle checkpoints, and DNA repair [13,14]. DDR can lead to cell rescue by means of DNA repair, to permanent growth arrest, *i.e.* cell senescence, or to cell death through apoptosis [14,15]. The less abundant Pt-interstrand-DNA adducts prompt the DDR [16]. In fact, they are processed to double strand breaks (DSB), that trigger PI3 kinases (as ATM) signaling.

ATM expression is ruled by the E2F-1 transcription factor [17], a c-Myc target gene [18]. ATM is activated by oxidative stress-sensors as HO-1 [19]. Cisplatin treatment induces HO-1 expression [20]. ATM phosphorylates the downstream players p53 and γH2AX and thus induces the DDR [13].

The transcription factor p53 responds to cellular stress regulating target genes able to induce cell cycle arrest, senescence, DNA repair [21] (as GADD45 [22]) and apoptosis (as APAF-1 [23]). The latter protein plays a central role in apoptosis induction as it activates procaspase-9, the upstream step of effector caspases [24]. However, p53-dependent apoptotic checkpoint depends on DAPK1 [25], and the downstream activity of caspase-3, -7 and -9 is blocked by members of the inhibitor of apoptosis (IAPs) family, as XIAP and survivin. These proteins are upregulated in mesothelioma, leading to cell survival [26].

γH2AX foci are platforms for the accumulation of DNA damage response and repair factors to the DSB site [27]. Homologous recombination (HR) and non-homologous end joining (NHEJ) are the main DNA repair mechanisms of DSBs [28]. In particular, HR mediates cisplatin resistance and represents the target for new therapies [29].

Cisplatin chemoresistance is directly linked to c-Myc [30], and c-Myc repression is synergistic with cisplatin in MPM treated cells [31]. The proto-oncogene c-myc encodes a transcription factor that plays a critical role in an epigenetic manner [32] over a broad range of cellular processes, including cell cycle progression, cell growth, differentiation, transformation, angiogenesis, apoptosis and chemoresistance [33].

Albeit modulation of c-Myc might enhance the response of cisplatin against MPM and possibly modulate its chemoresistance, targeting c-Myc causes heavy systemic effects in healthy tissues with high proliferative index [34]. However, c-Myc modulation can be selectively induced in cancer cells targeting the BET subfamily of bromodomain (BRD)-containing proteins. In particular, BRD4 is a ubiquitous transcription co-factor, associated with oncogenes, whose transcription is ruled by super-enhancers [35]. Super-enhancers need an excess of transcription, rendering the gene very sensitive to BRD4 inhibition. Since the survival of transformed cells depends on oncogenes, their depletion induces death preferentially in cancer cells, while preserving somatic ones [36]. BRD4 controls genes involved in cell proliferation, cell cycle progression, oxidative stress response, inflammation, and DNA repair [37]. These pathways are all deregulated in MPMs [38].

BET inhibitors are gaining increasing attention and some of them entered clinical trials [37]. Furthermore, they showed strong anti-inflammatory effects [39]: as far as immune-based therapies are gaining increasing attention for the treatment of mesothelioma [40], BET inhibitors could represent both anticancer and anti-inflammatory therapeutic approach. Thus, BRD4 inhibition could be a promising strategy against this kind of cancer.

JQ1, a thienodiazepine derivative, was developed as a specific BRD4 inhibitor [41, 42] and showed encouraging antitumor activity both *in vitro* and *in vivo*. It leads to repression of c-Myc and of c-Myc target genes by abrogating recruitment of enhancer complexes [43]. Combination of JQ1 and cisplatin resulted synergistic on animal models of ovarian cancer both *in vitro* and *in vivo*, [44] and showed similar effects on other cancer types [45, 46]. Furthermore, JQ1 enhances apoptosis induction in cisplatin-resistant cells [47].

Furthermore, JQ1 increases HO-1 [48], and BRD4 inhibition enhances the ATM-dependent DNA damage signaling and triggers DDR [49, 50].

Marked differences in JQ1 sensitivity correlate to modulation of another BRD4 target gene: Fra-1, also known as FOSL1 [51]. Fra-1 is an oncogenic transcription factor belonging to the Fos subfamily, that dimerize with Jun proteins to form AP-1, a transcription factor involved in mesothelial transformation [52]. AP-1 and c-Myc stimulate transcription of genes encoding proteins that promote progression through the G_1 phase of the cell cycle and the G_1 to S transition [53,54], and inhibit CDK inhibitor p21, mainly regulating its p53-directed transcription [55, 56]. Increased levels of p21 can lead to a permanent growth arrest, *i.e.* cellular senescence [57], and can be induced by both cisplatin [58-60] and JQ1 [61-64].

JQ1 induces p21 also in a p53-independent way, i.e. LATS1/YAP signaling inhibition [64]. YAP plays the central role of the Hippo pathway, a promising target for MPM therapy [65]. YAP induces c-Myc transcription, but c-Myc itself inhibits YAP, hence downregulated c-Myc could increase YAP-target genes transcription [66], as BIRC5/survivin [67], an inhibitor of apoptosis (IAP) member. On the other side, this gene can be inhibited by p21 along with p53 [57]. Survivin regulates tumor cell apoptosis via its interaction with XIAP [68], another BET target, that decreases upon JQ1 treatment [45].

Thus, JQ1 could decrease the antiapoptotic armory in MPM cells and lower the chemoresistance as well. With this goal, we investigated if JQ1 is able to inhibit MPM growth and thus, playing a role in combination chemotherapy of MPM.

2. MATERIALS AND METHODS

All compounds were tested on three MPM cell lines, called BR95 (epithelioid), MG06 (mixed or biphasic, with epithelioid predominance), MM98 (sarcomatoid), and a cisplatin-resistant cell line called MM98R. All cell lines were obtained from the biobank of the Hospital of Alessandria [10] and were routinely tested for mycoplasma contamination.

BR95 and MG06 cells were grown in F10 Ham medium, while DMEM was used for sarcomatoid cells. Media were supplemented with L-glutamine 2 mM, penicillin 100 IU mL^{-1}, streptomycin (100 mg L^{-1}) and 10% FBS, and cells were cultured at 37 °C in a 5% CO_2 humidified chamber.

2.1. Drug Screening Assays

A quantity of 2-5 $\times 10^3$ cells per well were seeded onto black sterile tissue-culture treated 96-well plates (CulturPlate 96 F, Perkin Elmer, Milan) and allowed to attach 24 hours before drug treatment.

Cisplatin was dissolved in 0.9% (w/v) NaCl aqueous solution brought to pH 3 with HCl (final stock concentration 1 mM). JQ1 was dissolved in DMSO to final concentration 10 mM. The final DMSO concentration never exceeded 0.5% (non-toxic concentration).

Combination experiments were carried on using fixed dose ratio protocols [69]. For simultaneous administration, cisplatin and JQ1 mother solutions were co-diluted (at molar ratio 1:10 for MM98 and MM98R cell, and at molar ratio 1:3 for BR95 and MG06, according to their relative drug sensitivity) and the resulting stock solution was serially diluted to a range of three orders of magnitude of concentrations and administered to cells.

Challenges were performed for 72 hours continuous treatment (CT). Residual cell viability was evaluated by means of the resazurin reduction assay, as previously reported [70]. Fluorescence was measured using an excitation wavelength of 550 nm and an emission wavelength of 585 nm with a Tecan Infinite F200Pro plate reader (Tecan Austria).

In each experiment, cells were challenged with the drugs at different concentrations and the final data were calculated from at least three replicates of the same experiment carried out in triplicate. The fluorescence intensities of 8 wells containing medium without cells were used as background value to be subtracted. Data were normalized to 100% cell viability for non-treated cells; IC_{50} (half inhibitory concentration) was obtained from the dose-response sigmoid using Origin Pro (version 8, Microcal Software, Inc., Northampton, MA, USA). Data presented were calculated from at least three replicates of the same experiment carried out in triplicate.

The combination index (CI) was calculated for non-mutually exclusive drugs, according to the following equation:

$$CI = \frac{D_1}{D_{x1}} + \frac{D_2}{D_{x2}} + \frac{D_1 \times D_2}{D_{x1} \times D_{x2}}$$

where D_{x1} and D_{x2} were the concentrations required for a given effect (the same residual cell viability *e.g.* 50% growth inhibition, IC_{50}) respectively for drug **1** and **2** alone, while D_1 and D_2 were the concentrations required for the same effect for drug **1** and **2** in a combination experiment. CI values below 1 indicated synergism, equal to 1 additive effect, and higher than 1 antagonism [71].

2.2. Immunoblot Analysis

BR95 and MG06 were treated with 2.5 μM JQ1, and/or with cisplatin at molar ratio 1:3, while MM98 and MM98R were treated for 24 h with 0.25 μM JQ1 and/or with cisplatin at molar ratio 1:10. Then, cells were lysed in RIPA buffer (50 mM Tris–HCl, 150 mM NaCl, 1% Igepal CA-630, 0.1% SDS, pH 8) supplemented with protease inhibitor cocktail (Sigma-Aldrich); after 3 cycles of freeze-thawing, cell debris were removed by centrifugation. Protein concentration was determined using the bicinchoninic acid method (BCA assay, Pierce Biotechnology). A total of 10 μg of proteins were run on a 10% SDS–PAGE, then blotted onto a PVDF membrane (Immobilon-P, Millipore, MA, USA), blocked with 3% w/v non-fat milk, and finally detected by Mouse anti c-Myc primary antibody (9E10: sc40, diluted 1:200), rabbit anti Fra-1 (R-20: sc-605, diluted 1:200), and mouse anti actin (C-2: sc-8432, diluted 1:200), and HRP-conjugated anti-mouse and anti-rabbit antibodies (sc-2005 and sc-2004, diluted 1:2000 and 1:5000, respectively). All antibodies were purchased from Santa Cruz Biotechnology. Blots were developed with ECL reagent (Sigma-Aldrich), using a ChemiDoc apparatus (Bio-Rad). Each experiment was repeated at least twice. A549 lung adenocarcinoma cells were used as positive control for the immunoblot analyses.

2.3. Cell Cycle Analysis

After the treatments performed as above, cells were fixed in 70% cold ethanol, and stored at -20°C. Before the analysis, cells were treated with 20 μg/ml RNAse A in PBS (for 30 min at room temperature), then diluted to $5x10^5$ cells/ml in PBS containing 50 μg/ml propidium iodide (PI). Flow cytometric analyses were performed with a Partec CyFlow Space (Partec GmbH, Muenster, Germany). Data were analyzed with the CyFlogic v 1.1.1. Data from two independent experiments, performed in duplicate, were compared to untreated control by means of a chi-squared test (* $p<0.05$; ** $p<0.01$; *** $p<0.001$).

2.4. Single Cell Gel Electrophoresis (SCGE), or Comet Assay

Cells were challenged with the drugs for 24 hours with the same concentrations as above. H_2O_2 was used as positive control (0.7 mM, 5 min treatment). A total of 250 $\times 10^3$ cells were mixed with an equal volume of 0.5% Low melting point agarose (LMA), and deposed onto the precoated slides with 1% normal melting point agarose (NMA). A final layer of LMA was added. Cell lysis was performed in 2.5 M NaCl, 100 mM EDTA, 10 mM Tris, 1% Triton X-100, pH 10 for 1 hour at 4 °C. Slides were then washed with water, and transferred to an electrophoresis tank for 10 min at room temperature in 300 mM EDTA, 300 mM NaOH, pH 13.0; then, a 10 min electrophoretic run (300 mA, 25 V) was performed [72]. Slides were neutralized with PBS, air-dried and fixed in ethanol. All buffers were freshly prepared prior use.

Nuclei were stained with 0.2 μg/ml DAPI. Digital images of the nuclei were recorded at 40X magnification (Axiocam and Axiovert, Carl Zeiss Inc., Thornwood, NY).

Three independent replicates were performed and a total of 50 cells were scored for each sample. The captured images were analyzed for the % DNA in tail (TI) with TriTek CometScore™. For each treatment, log-transformed TI values were compared to control by means of a two-sample t-test. Data (*i.e.* the median values, back-transformed to TI) were normalized *versus* the control, to calculate the fold-change, according to current guidelines [73].

2.5. Apoptosis: Caspase-3/7 Activity

The human ovarian carcinoma cell line A2780 was used as positive control for apoptosis induction [74] and the assay was performed similarly to a previous report [75]. A2780 cells were treated with 10 μM cisplatin or the same schedules as above. $1x10^4$ cells were seeded in 96-well tissue culture (TC) plates in complete medium, the day before treatment, performed with the same concentrations as above (and lower). After 24h, cells were washed, and lysed with 25 μL of lysis buffer (10 mM HEPES, 2 mM EDTA, 2 mM DTT, 0.1 % CHAPS, pH 7.4). The caspase 3/7 inhibitor Ac-DEVD-CHO 0.01 g/L (Sigma-Aldrich) was added to control wells. Then, 200 μL the caspase-3 fluorescent substrate, Ac-DEVD-AFC (Sigma-Aldrich), 0.01 g/L in lysis buffer, was added to all wells. A volume of 200 μL of each sample was transferred to a black microtiter plate and the activity was followed for 1 hour by means of fluorescence at Exc. 390/ Em. 520 nm, normalized *versus* the blank. Final fold activity (with respect to control wells) was calculated as the mean of at least three independent replicates performed in duplicate for each condition.

2.6. Detection of Cellular Senescence: Senescence-associated (SA) β-galactosidase Staining

The SA-β-galactosidase staining was performed as previously described [76]. BR95 and MG06 were treated with 0.5, 1 and 2.5 μM JQ1, and/or with cisplatin at molar ratio 1:3 MM98 and MM98R were treated with 0.05, 0.1 and 0.25 μM JQ1 and/or with cisplatin at molar ratio 1:10. After 3 days, a set of experiments was stopped by means of fixation in 3% formaldehyde, while drug-free fresh medium was given to a parallel set, and left until the 7^{th} day. At least three different 10X microscopic fields per well were photographed (Leica EC3 camera mounted on a Leica DMIL LED microscope), and the total number of cells and the blue ones was counted with the Cell Counter plug-in of ImageJ 1.45s.

2.7. 3D-spheroid Mesothelioma Model

Spheroids were adopted since they simulate better the diffusion gradient of drugs, O_2 and nutrients [77]. They were prepared following a previously published protocol [78]. Briefly, BR95 cells at 10^4 /well density were seeded in U-shaped 96-well polypropylene plates, and incubated on an orbital mixer in a standard culture incubator. After 4 days, spheroids of 300-400 μm diameter were obtained. Cisplatin was given for 24h, and then spheroids were treated with JQ1 for further 3 + 3 days. Control experiments were carried out with drug-free medium. On day 4 and 7 of treatment (corresponding to day 8 and 11 from cell seeding, day 0) were taken pictures of at least three spheroids *per* each experimental condition were taken at 4X magnification and the dimensions of spheroids were assessed using the Leica Application Suite software (v. 2.0). The spheroid volume was calculated from the mean diameter, and reported as fold change with respect to the time zero of the treatment.

2.8. Quantitative Real-time PCR (qPCR)

Total RNA was extracted by means of a kit (GenElute MAMMALIAN TOTAL RNA MINIPREP KIT), followed by DNAse treatment (DNAse I) (Fermentas, St. Leon-Rot, Germany). Then, 1 μg RNA was retrotranscribed in cDNA with the RevertAid™ H Minus First Strand cDNA Synthesis Kit (Thermo-Fisher) using the random primers. Each gene expression was normalized on the housekeeping gene ribosomal 18S rRNA. Assays were performed in triplicate for each treatment in a 20 μl reaction volume containing 1 μl of RT products, 10 μl Sso-Fast EVA Green SMX (Bio-Rad), 500 nM each forward and reverse primers, to detect c-Myc, Fra-1, Fos, HO-1, ATM, GADD45A, BIRC Surv, p21, p53,APAF-1, DAPK1, XIAP, as indicated in Table **S1.**

An automated CFX96 real-time thermocycler was used (Bio-Rad). The reaction conditions were 95°C for 1 minute, followed by 45 cycles 98°C for 5 seconds and anneal–extend step for 5 seconds at 60 °C, with data collection. At the end of these cycles, a melting curve (65°C to 95°C, with plate read every 0.5°C) was performed in order to assess the specificity of the amplification product by single peak melting temperature verification. Results were analyzed with Bio-Rad CFX Manager and exported to Excel (Microsoft, Redmond, WA, USA) for calculation and statistical analyses.

3. RESULTS AND DISCUSSION

3.1. JQ1 Enhances Cisplatin Cytotoxicity Inducing Apoptosis and Growth Arrest in MPM Cells

The MPM cells were challenged with JQ1 or cisplatin to observe the relative chemosensitivity (Table **1**). Among the different MPM phenotypes, MM98 and MM98R cells were the most sensitive to JQ1, with negligible difference for the cisplatin-resistant cell line, as previously observed for other cancer types [47].

We performed drug combination studies, employing cisplatin and JQ1 at fixed molar ratio, *i.e.* 10:1 on sarcomatoid cells and 3:1 on epithelial and mixed cells, chosen according to their IC_{50} values.

As shown in Fig. **1A-C**, the drug combination was always more active than cisplatin alone, and resulted synergistic on MG06 (CI<1, Fig. **1A** and **1B**), partially synergistic on MM98 (Fig. **1C** and **1D**), and additive on the remaining MPM cells (Fig. **1E-H**, CI around 1). Thus, drug synergism did not rely on cellular MPM phenotype and was unrelated to the cell-line chemosensitivity.

Superadditivity was observed after 3 days of treatment, based on residual viability, which depends on cell death and growth inhibition. Both phenomena occur at earlier time, thus we performed the specific assays after 24 hours of treatment with IC_{50}-value concentrations: BR95 and MG06 were treated with 2.5 μM JQ1, and/or with cisplatin at molar ratio 1:3, while MM98 and MM98R were treated with 0.25 μM JQ1 and/or with cisplatin at molar ratio 1:10.

Caspase 3/7 is the central player of both intrinsic and extrinsic apoptotic pathways, leading to cell death. As shown in Fig. (**2**), while cisplatin had negligible effect, JQ1 induced significant caspase-3/7 activation in all MPM cell lines. The combination further increased apoptosis in MG06 and MM98, correlating with the observed synergism. Thus, independently on the cellular chemosensitivity, JQ1 showed a remarkable pro-apoptotic activity.

Table 1. **IC_{50} values (intended as μM concentrations) obtained after 72h of treatment. Resistance Factor, RF = IC_{50} MM98R / IC_{50} MM98. Data are means ± standard deviation of at least 3 replicates.[a] Data previously published [9].**

	BR95	MG06	MM98	MM98R	
	IC_{50}(μM)				RF
JQ1	2.2±0.6	1.0±0.3	0.089 ±0.023	0.18±0.08	2.0
cisplatin	6.2±0.9	4.1±1.5 [a]	3.2±1.0 [a]	19.4±2.8 [a]	8.1 [a]

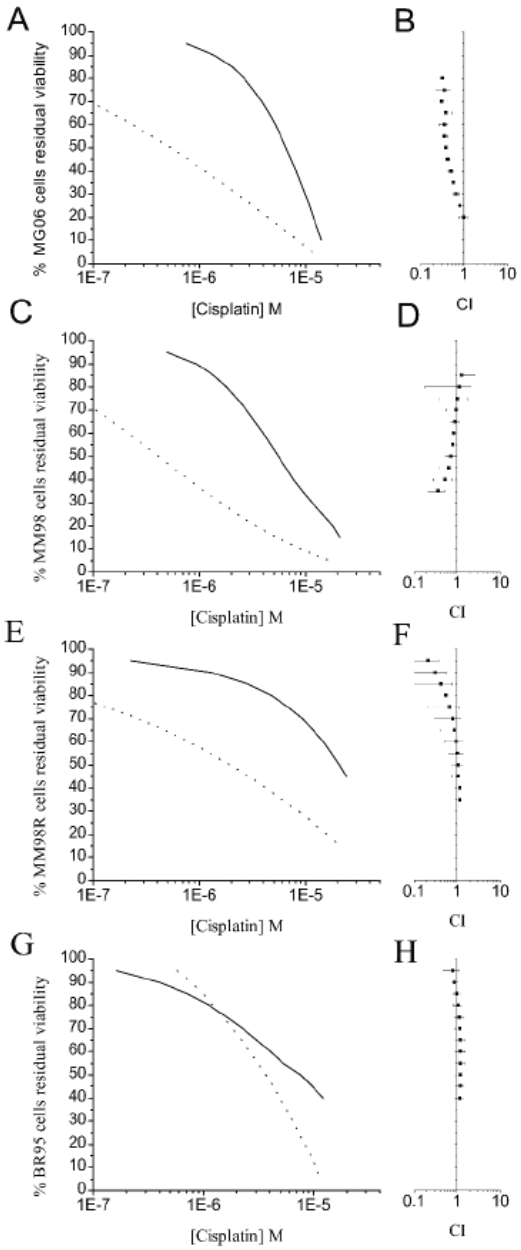

Fig. (1). Pharmacological interaction of JQ1 and cisplatin. Each row shows on the left the concentration-response graph of the cells challenged with cisplatin only (solid line) or cisplatin and JQ1 (dotted line). On the right, the combination index (CI) value computed for the same levels of residual viability is shown (A),(B): MG06; (C), (D): MM98; (E), (F): MM98R; (G), (H): BR95. Data are shown as the mean ± standard deviation of at least 3 replicates for each experiment.

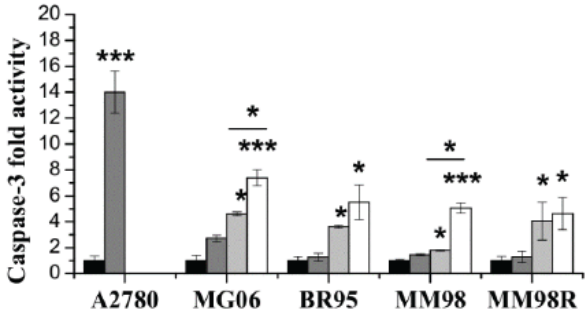

Fig. (2). Apoptosis induction after 24 h treatments. The positive control, A2780 cells, were treated with 10 μM cisplatin. Data are shown as Caspase 3/7 fold-change activity of treated cells over the untreated control (black filled bars), after cisplatin (grey bars), JQ1 (light grey bars), or the combination of both (white bars). Data are shown as the mean ± standard deviation. The statistic determination was computed *versus* the untreated control by means of two-sample t-test ($p<0.05$; ** $p<0.01$; *** $p<0.001$).

Cell cycle analyses gave contrasting results: as shown in Fig. (**3**), JQ1 had negligible effect on BR95 and MG06 cell cycle distribution, while induced G_1 arrest in the most sensitive MM98 and MM98R, as expected. Cisplatin increased the S phase in BR95, MG06 and MM98, but not MM98R. G_2 increased in MM98 only. Since successful DSB repair involves HR, a backup-copy of DNA, represented by a sister chromatid is essential; thus, HR is restricted to late S and G_2 phases of the cell cycle, as usually observed in cisplatin-treated cells [5].

Combination treatment allowed cells to recover the same pattern as the control, except MG06 and, partially, BR95, where the same pattern caused by cisplatin was observed ($p>0.05$).

We also observed late effects of the treatments on MPM cellular growth. The SA β-galactosidase staining was performed both after 3 days of treatment (T), and after further 4 days of recovery (R) in drug-free medium (3-T and 4-R, (Fig. **4**) left and right, respectively). The combination between JQ1 and cisplatin induced the highest percentage of senescence, both after 3-T and after additional 4-R. Few senescent cells (<20%, Fig. **4G-H**) were observed in MM98R after all treatments. The withdrawal of treatments (4-R) reduced senescent cells, in MM98 in more evident manner (Fig. **4F**). Thus, growth inhibition needed a prolonged exposure.

Since cisplatin is usually given as a bolus injection or as infusions varying from 1 hour to 24 hours [79], while a prolonged JQ1 treatment is safe [80], we tested a schedule

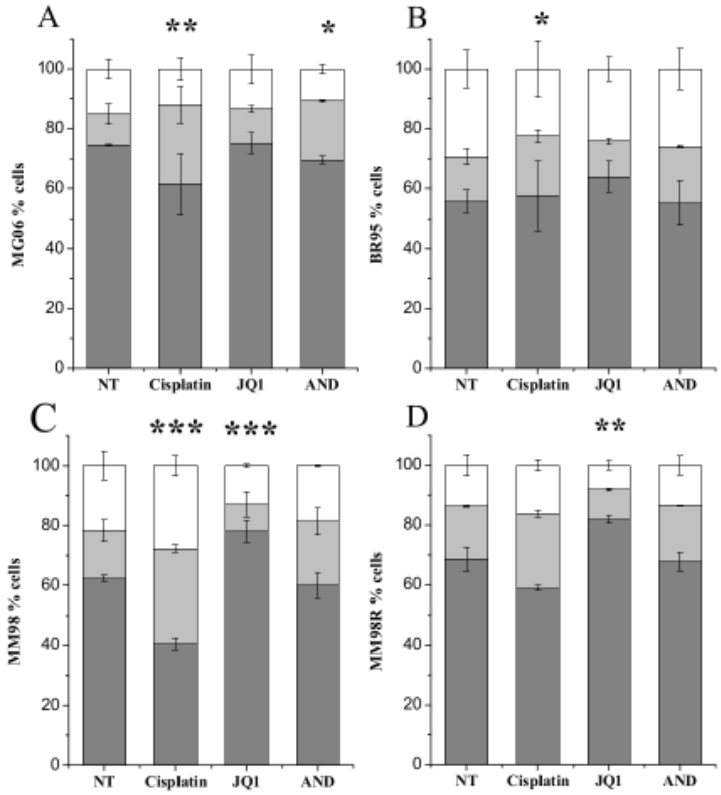

Fig. (3). Cell cycle distribution after 24 hours treatment of (A) MG06; (B) BR95; (C) MM98; (D) MM98R. Stacked columns represent the % of cells attributed to each cell cycle phases (dark grey: G1, light grey: S, white: G2/M). Data are shown as the mean ± standard deviation, and compared to untreated control by means of a chi-squared test (* $p<0.05$; ** $p<0.01$; *** $p<0.001$).

consisting of prolonged treatment with JQ1 after cisplatin. When BR95 spheroids were challenged with cisplatin for 24 hours and with JQ1 for further 6 days, strong volume decrease was observed even at low micromolar concentrations of both drugs, as shown in Fig. **5** and Fig. **S1**.

Data show that cisplatin activity on MPM is mainly antiproliferative: it induces no apoptosis (Fig. **2**), but S phase cell cycle arrest (Fig. **3**) and cellular senescence (Fig. **4**), except for the cisplatin-resistant sub-line, MM98R. On the contrary, JQ1 is proapoptotic in all MPM cell lines, with a modest antiproliferative activity. Apoptosis induction may be the mechanism underlying the observed superadditivity.

3.2. The Role of BRD4-related Pathways

JQ1 activity on cancer cells has been mainly attributed to c-Myc [41] or to FOSL1 [47] decrease. Thus, these BRD4 target proteins were quantified by immunoblotting (Fig. **6**). As expected, JQ1 decreased c-Myc expression in all MPM models, except for the cisplatin-resistant cell line MM98R, where a cisplatin-induced increase of c-Myc was observed (Fig. **6A**). The simultaneous treatment with JQ1 reversed this trend, as it downregulated c-Myc in all MPM cells (Fig. **6B**).

As Fig. (**6A**) shows, A549 lung cancer cells were used as positive control for the immunoblot and gave an intense band around 40 kDa, and a faint band around 30 kDa (Fig. **6C**), assigned to the phosphorylated and the unmodified protein, respectively. Only the latter band was observed in MPM. The expression of Fra-1 decreased in epithelial-like cells (MG06 and BR95) after JQ1 and combination treatment (Fig. **6C**). Thus, Fra-1 downregulation could somewhat contribute to the chemosensitization activity of JQ1.

The pattern of expression of the two c-Myc and Fra-1 transcripts was assayed by means of qPCR, along with other BRD4-related target genes.

As shown in Fig. (**7**), c-Myc mRNA decreased on all cell lines after JQ1 treatment, but not in MM98 and MM98R after cisplatin treatment, as observed for the expressed proteins. Furthermore, the combination induced a slight increase of c-Myc mRNA expression. Thus, while JQ1 showed a canonical c-Myc decrease on epithelial-like cells BR95 and MG06, it had contrasting effects on c-Myc levels on the sarcomatoid MPM cells.

Fra-1 expression dropped in all cell lines after JQ1 treatment, except for the cisplatin-resistant sub-line MM98R, and for the combination with cisplatin, that induced a Fra-1 increase in both MM98 and MM98R.

As shown in Fig. (**7**), Fos expression varied independently on Fra-1 in a cell-line-dependent fashion, with an evident reduction in MM98 and an increase in the epithelioid cell lines (BR95 and MG06).

3.3. The Role of p53 and p21

As expected, low levels of c-Myc and Fra-1 induced p53 and p21 expression after cisplatin treatment in all MPM cell lines (Fig. **7**). On the contrary, JQ1, both alone and in combination, induced p21 increase along with p53 decrease, as previously observed in other types of cancer [81] Upregulated

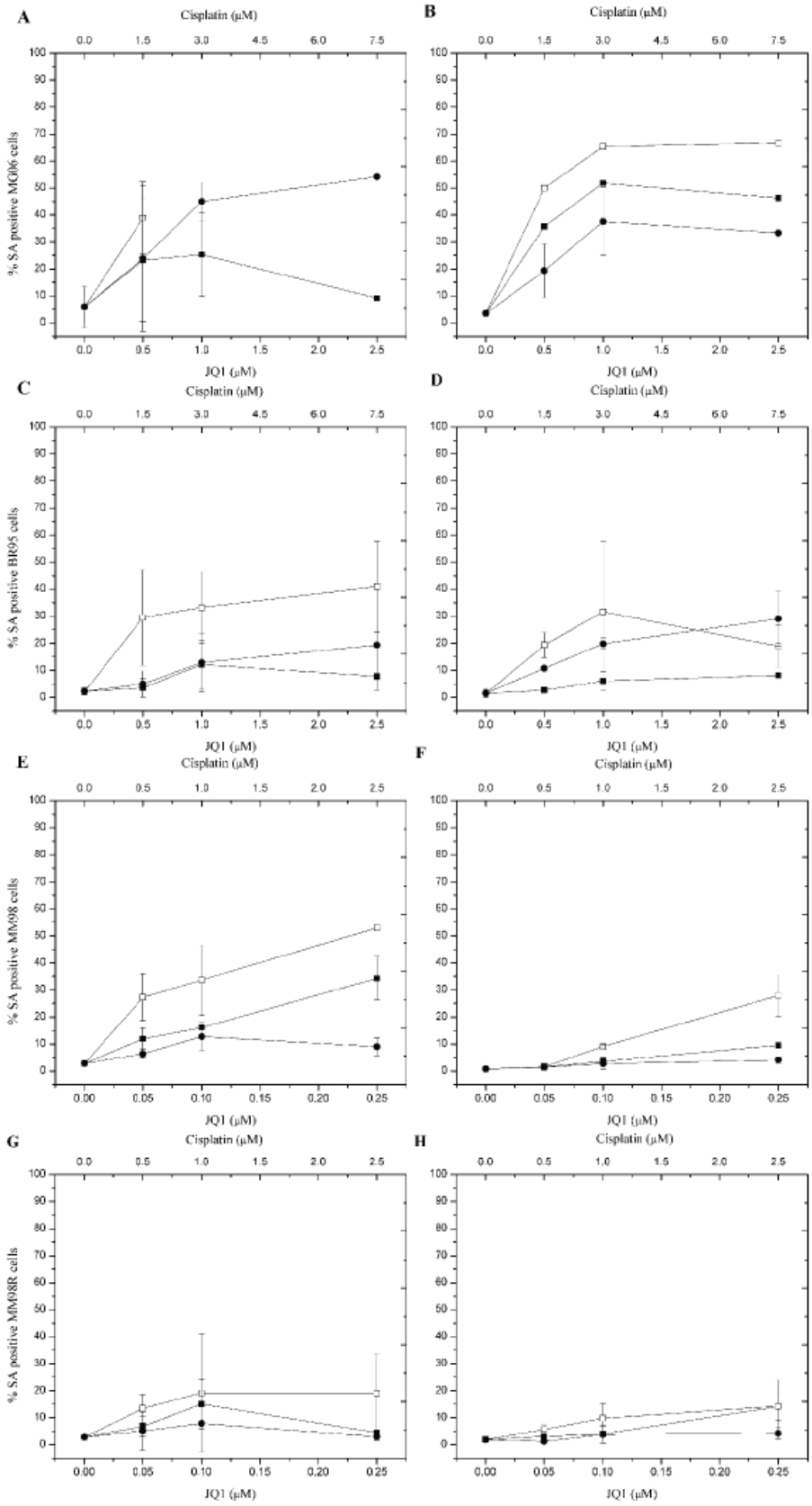

Fig. (4). Cell senescence was determined as the % of SA-β-gal positive (senescent) cells. Data are presented as the mean ± standard deviation of two independent replicates. The left side shows the assay performed after 3 days of treatment, while the right side shows the assay performed after further 4 days of recovery. From top to bottom: (A), (B): MG06; (C), (D): BR95; (E), (F): MM98; (G), (H): MM98R. Cisplatin (concentration given in the top axis): back filled circles; JQ1 (concentration given in the bottom axis): filled squares; cisplatin+JQ1: white squares.

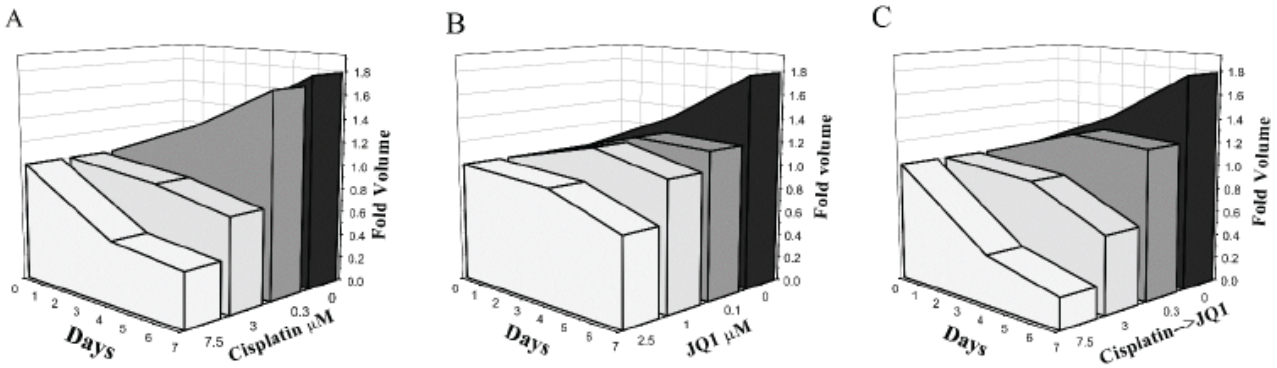

Fig. (5). BR95 spheroids growth inhibition. (A) treatment with cisplatin for 1 day, followed by drug-free medium for 3+3 days. (B) treatment with drug-free medium for 1 day, followed by JQ1 for 3+3 days (C) treatment with cisplatin for 1 day, followed by JQ1 for 3+3 days.

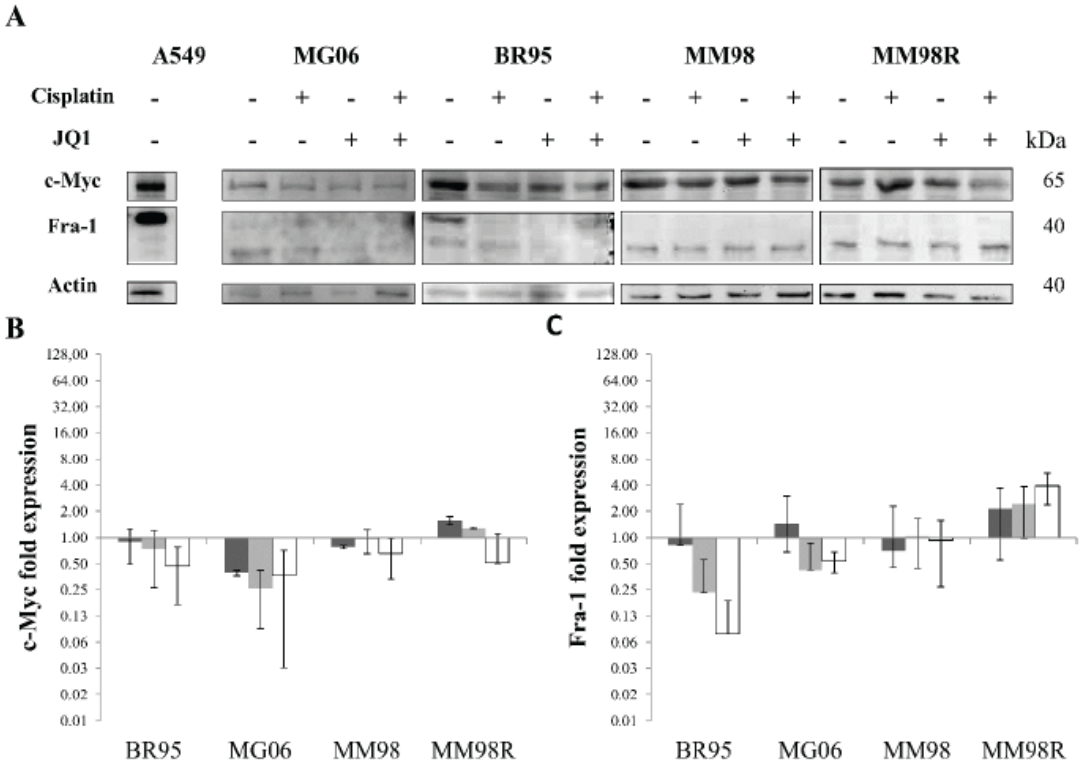

Fig. (6). Expression of target proteins c-Myc and Fra-1 after 24 h treatments. (A) Representative immunoblots for c-Myc, Fra-1 and loading control (actin). (B) log2 fold increase of c-Myc with respect to the untreated control. (C) log2 fold increase of Fra-1 with respect to the untreated control after cisplatin (grey bars), JQ1 (light grey bars), or the combination of both (white bars). Data are shown as the mean ± standard deviation.

p21 correlated with senescence induction, showing the maximal effect after the combination treatment (Fig. **4**). p21 levels were increased in cells where JQ1 induced G_1 arrest, namely MM98 and MM98R (Fig. **7** and Fig. **3 C-D**), as previously reported [47].

Downstream genes as BIRC5/survivin were actually modulated by JQ1, and by cisplatin, with cell-line-specific patterns (Fig. 7). Furthermore, following JQ1-based treatments, all MPM cell lines showed decreased XIAP transcript, except MM98R and cisplatin-treated BR95 cells.

The pattern of expression of p53, XIAP and APAF-1 were similar in all MPM cell lines, except for BR95 cells, that express a mutant p53 protein [5,82]. APAF-1 expression was marginally affected by cisplatin treatment, and increased in BR95 and MM98R; on the contrary, JQ1 and its combination decreased APAF-1 in MM98 and MG06 cells, where synergism was observed (Fig. **1**).

Therefore, in MPM cells JQ1–induced apoptosis mostly relied on c-Myc downregulation rather than that of p53. JQ1 and/or its combination treatment favored apoptosis induction modulating proapopototic (APAF-1, DAPK) and antiapoptotic genes (IAPs).

3.4. The Role of DNA Damage and Repair

As expected, ATM and c-Myc expression exhibited a similar pattern in all MPM cell lines (Fig. **7**). The increased expression of HO-1 likely activated ATM, except in MM98 cells (Fig. **7**).

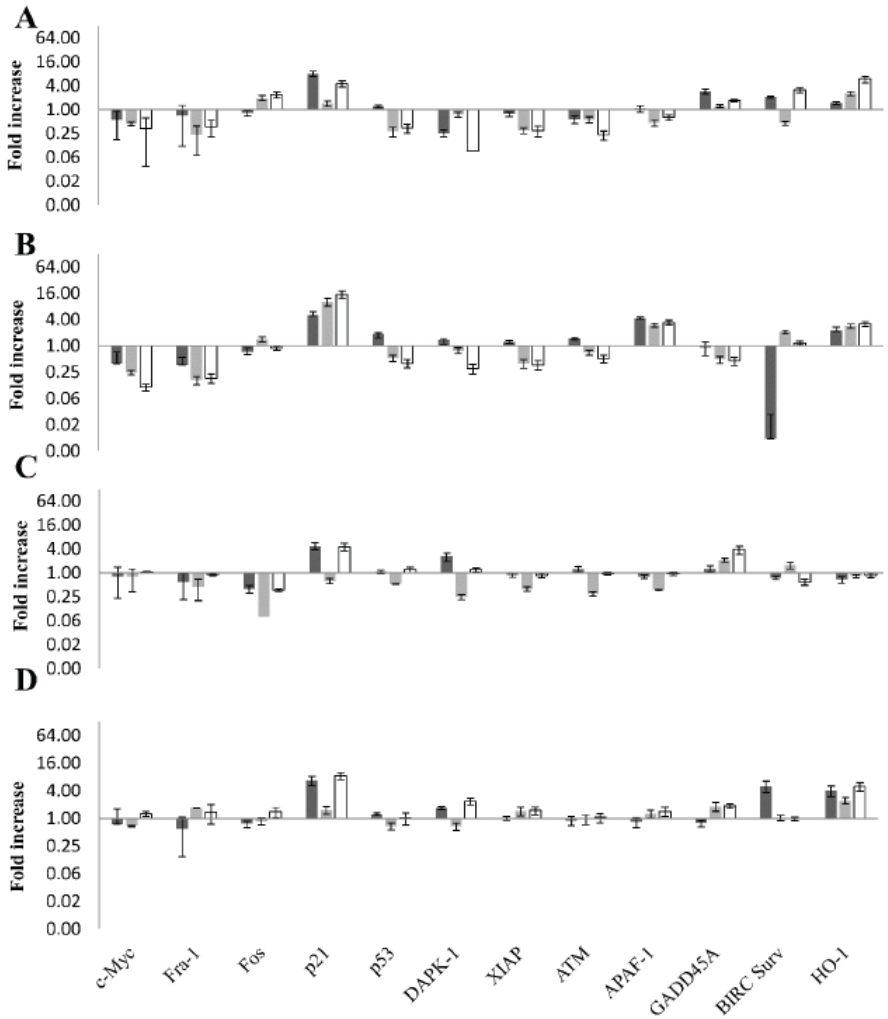

Fig. (7). qPCR measure of expression levels of selected target genes, after a 24 hours treatment. Bars represent the log2 fold increase *versus* the untreated control (dark grey: cisplatin, light grey: JQ1, white: combination). (A) MG06; (B) BR95; (C) MM98; (D) MM98R. Bars represent mean values ± standard deviation.

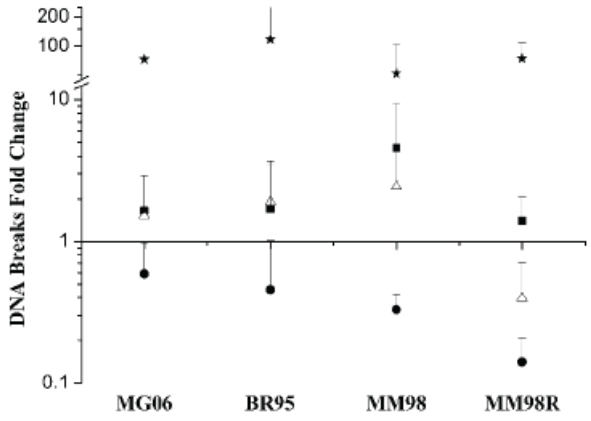

Fig. (8). DNA breaks induced by the treatments. Data are shown as the mean ± standard deviation of fold median TI variation, *versus* the untreated control, represented by the horizontal line at value 1. Filled squares: cisplatin; filled circles: JQ1; open triangles cisplatin+JQ1; filled stars: positive control (H_2O_2).

ATM activates p53, a central protein in apoptosis induction, cellular senescence and DNA repair.

The p53-dependent apoptotic checkpoint relies on DAPK1, and it is turned on by c-Myc [25]. Accordingly, the pattern of expression of DAPK1 and p53 were similar to that of c-Myc after JQ1-based treatments (Fig. **7**).

p53 rules the expression of GADD45 [22], which stimulates NER [83]. GADD45 was upregulated by cisplatin treatments, except in the resistant cell line MM98R (Fig. **7**), probably due to increased tolerance to Pt-DNA adducts. However, except in p53-defective BR95 cells, JQ1 alone or its combination treatment induced GADD45 expression.

As previously stated, Pt-DNA adducts are processed to SSBs and to DSBs. Accumulation of DNA breaks suggests tolerance to Pt-DNA adducts or uncompleted damage process. The comet assay should evidence such DNA breaks. As (Fig. **8** and Fig. **S2**) shows, cisplatin induced a biologically relevant increase of DNA breaks (≥3 fold over control) in MM98 cells, indicating that active removal of DNA-Pt adducts was followed by uncompleted DNA repair. Accordingly, only MM98 cells showed G_2 phase increase after cisplatin treatment (Fig. **3C**), pointing out uncompleted DSB repair through HR. DNA breaks accumulation may explain the high cisplatin-sensitivity of these cells (Table **1**). Since

MM98 cells did not upregulate HO-1 expression (Fig. **7**), they were less able to induce an ATM-dependent DDR and proficient DNA repair. Senescence is a hallmark of the DDR-induced cellular fates [77,80]. Accordingly, treatment withdrawal (4-R) (Fig. **4F**) reduced cellular senescence in MM98 cells only, pointing out decreasing DDR signaling.

On the other hand, the other MPM cell lines increased HO-1 expression (Fig. **7**), showed relevant levels of senescence (Fig. **4**).

JQ1 reduced cisplatin-induced DNA breaks in MM98 and MM98R cells, and significantly reduced ($p<0.01$) basal DNA breaks in all MPM cells. These data are in tune with previous reports that showed that JQ1-dependent BRD4 inhibition enhances the ATM-dependent DNA damage signaling and triggers DDR [73,74].

CONCLUSION

The BET inhibitor JQ1 and cisplatin showed additive/superadditive efficacy on MPM cellular models. Their mechanisms of action complemented each other. In fact, JQ1 was able to enhance cisplatin activity by means of c-Myc downregulation. The consequent DDR enhancement lead to apoptosis induction and/or permanent growth arrest (senescence), depending on the MPM cellular context.

Both cellular fates represent a permanent antitumor effect, leading to tumor regression, at least in the 3D *in vitro* model. Thus, the pharmacological modulation of BET activity could represent a promising tool for future MPM therapy.

LIST OF ABBREVIATIONS

AP-1 = Activator Protein-1

APAF-1 = Apoptotic protease activating factor 1

ATM = Ataxia-telangiectasia mutated gene

BET = Bromodomain and extraterminal

BIRC5 = Baculoviral IAP Containing Protein 5

BRD = Bromodomain

CDK = Cyclin-dependent kinase

CI = Combination index

cisplatin = Cis-diamminedichloridoplatinum(II)

CO = Carbon monoxide

CT = Continuous treatment

DAPK-1 = Death-associated protein kinase

DDR = DNA Damage Response

DMEM = Dulbecco Modified Eagle's Medium

DSB = Double strand breaks

FBS = Fetal bovine serum

FOSL1 = FOS-Like antigen 1

GADD45/GADD45A = Growth arrest- and DNA damage-inducible gene A

HO-1 = Haem Oxygenase 1

HR = Homologous recombination

IAP = Inhibitor apoptosis

IC_{50} = Half inhibitory concentration

JQ1 = (+)-JQ1, namely S)-tert-butyl 2-(4-(4-chlorophenyl)-2,3,9-trimethyl-6H-thieno[3,2-f][1,2,4]triazolo[4,3-a][1,4]diazepin-6-yl)acetate

LATS1 = Large Tumor Suppressor 1

LMA = Low melting point agarose

MPM = Malignant Pleural mesothelioma

NER = Nucleotide Excision Repair

NHEJ = Non-homologous end joining

NMA = Normal melting point agarose

NRF2 = NFE2 related factor

p21 = $p21^{WAF1/Cip1}$

PI = Propidium iodide

PVDF = Polyvinylidene fluoride

qPCR = Quantitative real-time PCR

RIPA = Radio immune-precipitation assay

ROS = Reactive oxygen species

RT = Retrotranscription

SA-β-galactosidase = Senescence-associated (SA) β-galactosidase

SCGE = Single cell gel electrophoresis

SDS = Sodium dodecyl sulfate

SSB = Single strand breaks

TC = Tissue Culture

TI = Tail Intensity

YAP = Yes Associated Protein

ETHICS APPROVAL AND CONSENT TO PARTICIPATE

Not applicable.

HUMAN AND ANIMAL RIGHTS

No Animals/Humans were used for studies that are base of this research.

CONSENT FOR PUBLICATION

Not applicable.

CONFLICT OF INTEREST

The authors declare no conflict of interest, financial or otherwise.

ACKNOWLEDGEMENTS

We are indebted to Prof. S. Knapp (University of Oxford) for kindly providing us JQ1 and to the Alessandria Hospital Mesothelioma Biobank for providing us MPM cell lines. We thank Drs. Nadia Massa, Marta Boeri and Ilaria Bonarrigo (Università del Piemonte Orientale) for technical help in the experiments.

This research is supported by the Compagnia di San Paolo, research project "BIPLANES". We are indebted to Inter-University Consortium for Research on the Chemistry of Metals in Biological Systems (CIRCMSB, Bari) and UE COST CM1105 Action "Functional metal complexes that bind to biomolecules" for stimulating discussions during the group meetings and short-term missions.

SUPPLEMENTARY MATERIAL

Supplementary material is available on the publishers web site along with the published article.

REFERENCES

[1] Cao, C.; Tian, D.; Manganas, C.; Matthews, P.; Yan, T. D. Systematic Review of Trimodality Therapy for Patients with Malignant Pleural Mesothelioma. *Ann. Cardiothorac. Surg.* **2012**, *1* (4), 428–437.

[2] Kotova, S.; Wong, R. M.; Cameron, R. B. New and Emerging Therapeutic Options for Malignant Pleural Mesothelioma: Review of Early Clinical Trials. *Cancer Manag. Res.* **2015**, *7*, 51–63.

[3] de Assis, L. V. M.; Locatelli, J.; Isoldi, M. C. The Role of Key Genes and Pathways Involved in the Tumorigenesis of Malignant Mesothelioma. *Biochim. Biophys. Acta BBA - Rev. Cancer* **2014**, *1845* (2), 232–247.

[4] Remon, J.; Reguart, N.; Corral, J.; Lianes, P. Malignant Pleural Mesothelioma: New Hope in the Horizon with Novel Therapeutic Strategies. *Cancer Treat. Rev.* **2015**, *41* (1), 27–34.

[5] Zanellato, I.; Boidi, C. D.; Lingua, G.; Betta, P.-G.; Orecchia, S.; Monti, E.; Osella, D. *In Vitro* Anti-Mesothelioma Activity of Cisplatin-Gemcitabine Combinations: Evidence for Sequence-Dependent Effects. *Cancer Chemother. Pharmacol.* **2011**, *67* (2), 265–273.

[6] Alessio, M.; Zanellato, I.; Bonarrigo, I.; Gabano, E.; Ravera, M.; Osella, D. Antiproliferative Activity of Pt(IV)-Bis(carboxylato) Conjugates on Malignant Pleural Mesothelioma Cells. *J. Inorg. Biochem.* **2013**, *129*, 52–57.

[7] Margiotta, N.; Ostuni, R.; Piccinonna, S.; Natile, G.; Zanellato, I.; Boidi, C. D.; Bonarrigo, I.; Osella, D. Platinum-Bisphosphonate Complexes Have Proven to Be Inactive Chemotherapeutics Targeted for Malignant Mesothelioma because of Inappropriate Hydrolysis. *J. Inorg. Biochem.* **2011**, *105* (4), 548–557.

[8] Ravera, M.; Gabano, E.; Zanellato, I.; Bonarrigo, I.; Escribano, E.; Moreno, V.; Font-Bardia, M.; Calvet, T.; Osella, D. Synthesis, Characterization and Antiproliferative Activity on Mesothelioma Cell Lines of Bis(carboxylato)platinum(iv) Complexes Based on Picoplatin. *Dalton Trans. Camb. Engl. 2003* **2012**, *41* (11), 3313–3320.

[9] Zanellato, I.; Bonarrigo, I.; Gabano, E.; Ravera, M.; Margiotta, N.; Betta, P.-G.; Osella, D. Metallo-Drugs in the Treatment of Malignant Pleural Mesothelioma. *Inorganica Chim. Acta* **2012**, *393*, 64–74.

[10] Zanellato, I.; Bonarrigo, I.; Ravera, M.; Gabano, E.; Gust, R.; Osella, D. The Hexacarbonyldicobalt Derivative of Aspirin Acts as a CO-Releasing NSAID on Malignant Mesothelioma Cells. *Met. Integr. Biometal Sci.* **2013**, *5* (12), 1604–1613.

[11] Cepeda, V.; Fuertes, M. A.; Castilla, J.; Alonso, C.; Quevedo, C.; Pérez, J. M. Biochemical Mechanisms of Cisplatin Cytotoxicity. *Anticancer Agents Med. Chem.* **2007**, *7* (1), 3–18.

[12] Sertic, S.; Pizzi, S.; Lazzaro, F.; Plevani, P.; Muzi-Falconi, M. NER and DDR: Classical Music with New Instruments. *Cell Cycle Georget. Tex* **2012**, *11* (4), 668–674.

[13] Roos, W. P.; Kaina, B. DNA Damage-Induced Cell Death: From Specific DNA Lesions to the DNA Damage Response and Apoptosis. *Cancer Lett.* **2013**, *332* (2), 237–248.

[14] Rodier, F.; Muñoz, D. P.; Teachenor, R.; Chu, V.; Le, O.; Bhaumik, D.; Coppé, J.-P.; Campeau, E.; Beauséjour, C. M.; Kim, S.-H.; Davalos, A. R.; Campisi, J. DNA-SCARS: Distinct Nuclear Structures That Sustain Damage-Induced Senescence Growth Arrest and Inflammatory Cytokine Secretion. *J. Cell Sci.* **2011**, *124* (Pt 1), 68–81.

[15] Fumagalli, M.; d'Adda di Fagagna, F. SASPense and DDRama in Cancer and Ageing. *Nat. Cell Biol.* **2009**, *11* (8), 921–923.

[16] Woods, D.; Turchi, J. J. Chemotherapy Induced DNA Damage Response: Convergence of Drugs and Pathways. *Cancer Biol. Ther.* **2013**, *14* (5), 379–389.

[17] Berkovich, E.; Ginsberg, D. ATM Is a Target for Positive Regulation by E2F-1. *Oncogene* **2003**, *22* (2), 161–167.

[18] Leone, G.; Sears, R.; Huang, E.; Rempel, R.; Nuckolls, F.; Park, C.-H.; Giangrande, P.; Wu, L.; Saavedra, H. I.; Field, S. J.; Thompson, M. A.; Yang, H.; Fujiwara, Y.; Greenberg, M. E.; Orkin, S.; Smith, C.; Nevins, J. R. Myc Requires Distinct E2F Activities to Induce S Phase and Apoptosis. *Mol. Cell* **2001**, *8* (1), 105–113.

[19] Otterbein, L. E.; Hedblom, A.; Harris, C.; Csizmadia, E.; Gallo, D.; Wegiel, B. Heme Oxygenase-1 and Carbon Monoxide Modulate DNA Repair through Ataxia-Telangiectasia Mutated (ATM) Protein. *Proc. Natl. Acad. Sci. U. S. A.* **2011**, *108* (35), 14491–14496.

[20] Schaaf, G. J.; Maas, R. F. M.; de Groene, E. M.; Fink-Gremmels, J. Management of Oxidative Stress by Heme Oxygenase-1 in Cisplatin-Induced Toxicity in Renal Tubular Cells. *Free Radic. Res.* **2002**, *36* (8), 835–843.

[21] Vousden, K. H.; Lane, D. P. p53 in Health and Disease. *Nat. Rev. Mol. Cell Biol.* **2007**, *8* (4), 275–283.

[22] Kearsey, J. M.; Coates, P. J.; Prescott, A. R.; Warbrick, E.; Hall, P. A. Gadd45 Is a Nuclear Cell Cycle Regulated Protein Which Interacts with p21Cip1. *Oncogene* **1995**, *11* (9), 1675–1683.

[23] Robles, A. I.; Bemmels, N. A.; Foraker, A. B.; Harris, C. C. APAF-1 Is a Transcriptional Target of p53 in DNA Damage-Induced Apoptosis. *Cancer Res.* **2001**, *61* (18), 6660–6664.

[24] Bratton, S. B.; Salvesen, G. S. Regulation of the Apaf-1-Caspase-9 Apoptosome. *J. Cell Sci.* **2010**, *123* (Pt 19), 3209–3214.

[25] Raveh, T.; Droguett, G.; Horwitz, M. S.; DePinho, R. A.; Kimchi, A. DAP Kinase Activates a p19ARF/p53-Mediated Apoptotic Checkpoint to Suppress Oncogenic Transformation. *Nat. Cell Biol.* **2001**, *3* (1), 1–7.

[26] Zaffaroni, N.; Costa, A.; Pennati, M.; De Marco, C.; Affini, E.; Madeo, M.; Erdas, R.; Cabras, A.; Kusamura, S.; Baratti, D.; Deraco, M.; Daidone, M. G. Survivin Is Highly Expressed and Promotes Cell Survival in Malignant Peritoneal Mesothelioma. Cell. Oncol. 2007, 29 (6), 453–466.

[27] Bonner, W. M.; Redon, C. E.; Dickey, J. S.; Nakamura, A. J.; Sedelnikova, O. A.; Solier, S.; Pommier, Y. GammaH2AX and Cancer. *Nat. Rev. Cancer* 2008, 8 (12), 957–967.

[28] Fu, D.; Calvo, J. A.; Samson, L. D. Balancing Repair and Tolerance of DNA Damage Caused by Alkylating Agents. *Nat. Rev. Cancer* **2012**, *12* (2), 104–120.

[29] Muggia, F.; Safra, T. "BRCAness" and Its Implications for Platinum Action in Gynecologic Cancer. *Anticancer Res* **2014**, *34* (2), 551–556.

[30] Ganesan, S. MYC, PARP1, and Chemoresistance: BIN There, Done That? *Sci. Signal.* **2011**, *4* (166), pe15.

[31] Kitamura, A.; Matsushita, K.; Takiguchi, Y.; Shimada, H.; Tada, Y.; Yamanaka, M.; Hiroshima, K.; Tagawa, M.; Tomonaga, T.; Matsubara, H.; Inoue, M.; Hasegawa, M.; Sato, Y.; Levens, D.; Tatsumi, K.; Nomura, F. Synergistic Effect of Non-Transmissible Sendai Virus Vector Encoding the c-Myc Suppressor FUSE-Binding Protein-Interacting Repressor plus Cisplatin in the Treatment of Malignant Pleural Mesothelioma. *Cancer Sci.* **2011**, *102* (7), 1366–1373.

[32] Lüscher, B.; Vervoorts, J. Regulation of Gene Transcription by the Oncoprotein MYC. *Gene* **2012**, *494* (2), 145–160.

[33] Shen, D.-W.; Pouliot, L. M.; Hall, M. D.; Gottesman, M. M. Cisplatin Resistance: A Cellular Self-Defense Mechanism Resulting from Multiple Epigenetic and Genetic Changes. *Pharmacol. Rev.* **2012**, *64* (3), 706–721.

[34] Soucek, L.; Whitfield, J.; Martins, C. P.; Finch, A. J.; Murphy, D. J.; Sodir, N. M.; Karnezis, A. N.; Swigart, L. B.; Nasi, S.; Evan, G.

I. Modelling Myc Inhibition as a Cancer Therapy. *Nature* **2008**, *455* (7213), 679–683.

[35] Lovén, J.; Hoke, H. A.; Lin, C. Y.; Lau, A.; Orlando, D. A.; Vakoc, C. R.; Bradner, J. E.; Lee, T. I.; Young, R. A. Selective Inhibition of Tumor Oncogenes by Disruption of Super-Enhancers. *Cell* **2013**, *153* (2), 320–334.

[36] Villicaña, C.; Cruz, G.; Zurita, M. The Basal Transcription Machinery as a Target for Cancer Therapy. *Cancer Cell Int.* **2014**, *14* (1), 18.

[37] Mertz, J. A.; Conery, A. R.; Bryant, B. M.; Sandy, P.; Balasubramanian, S.; Mele, D. A.; Bergeron, L.; Sims, R. J., 3rd. Targeting MYC Dependence in Cancer by Inhibiting BET Bromodomains. *Proc. Natl. Acad. Sci. U. S. A.* **2011**, *108* (40), 16669–16674.

[38] Mossman, B. T.; Shukla, A.; Heintz, N. H.; Verschraegen, C. F.; Thomas, A.; Hassan, R. New Insights into Understanding the Mechanisms, Pathogenesis, and Management of Malignant Mesotheliomas. *Am. J. Pathol.* **2013**, *182* (4), 1065–1077.

[39] Nicodeme, E.; Jeffrey, K. L.; Schaefer, U.; Beinke, S.; Dewell, S.; Chung, C.-W.; Chandwani, R.; Marazzi, I.; Wilson, P.; Coste, H.; White, J.; Kirilovsky, J.; Rice, C. M.; Lora, J. M.; Prinjha, R. K.; Lee, K.; Tarakhovsky, A. Suppression of Inflammation by a Synthetic Histone Mimic. *Nature* **2010**, *468* (7327), 1119–1123.

[40] Marcq, E.; Pauwels, P.; van Meerbeeck, J. P.; Smits, E. L. J. Targeting Immune Checkpoints: New Opportunity for Mesothelioma Treatment? *Cancer Treat. Rev.* **2015**, *41* (10), 914–924.

[41] Filippakopoulos, P.; Knapp, S. Targeting Bromodomains: Epigenetic Readers of Lysine Acetylation. *Nat. Rev. Drug Discov.* **2014**, *13* (5), 337–356.

[42] Filippakopoulos, P.; Qi, J.; Picaud, S.; Shen, Y.; Smith, W. B.; Fedorov, O.; Morse, E. M.; Keates, T.; Hickman, T. T.; Felletar, I.; Philpott, M.; Munro, S.; McKeown, M. R.; Wang, Y.; Christie, A. L.; West, N.; Cameron, M. J.; Schwartz, B.; Heightman, T. D.; La Thangue, N.; French, C. A.; Wiest, O.; Kung, A. L.; Knapp, S.; Bradner, J. E. Selective Inhibition of BET Bromodomains. *Nature* **2010**, *468* (7327), 1067–1073.

[43] Qi, J. Bromodomain and Extraterminal Domain Inhibitors (BETi) for Cancer Therapy: Chemical Modulation of Chromatin Structure. *Cold Spring Harb. Perspect. Biol.* **2014**, *6* (12), a018663.

[44] Yokoyama, Y.; Zhu, H.; Lee, J. H.; Kossenkov, A. V.; Wu, S. Y.; Wickramasinghe, J. M.; Yin, X.; Palozola, K. C.; Gardini, A.; Showe, L. C.; Zaret, K. S.; Liu, Q.; Speicher, D.; Conejo-Garcia, J. R.; Bradner, J. E.; Zhang, Z.; Sood, A. K.; Ordog, T.; Bitler, B. G.; Zhang, R. BET Inhibitors Suppress ALDH Activity by Targeting ALDH1A1 Super-Enhancer in Ovarian Cancer. *Cancer Res.* **2016**, *76* (21), 6320–6330.

[45] Klingbeil, O.; Lesche, R.; Gelato, K. A.; Haendler, B.; Lejeune, P. Inhibition of BET Bromodomain-Dependent XIAP and FLIP Expression Sensitizes KRAS-Mutated NSCLC to pro-Apoptotic Agents. *Cell Death Dis.* **2016**, *7* (9), e2365.

[46] Zhang, L.; Tong, Y.; Zhang, X.; Pan, M.; Chen, S. Arsenic Sulfide Combined with JQ1, Chemotherapy Agents, or Celecoxib Inhibit Gastric and Colon Cancer Cell Growth. *Drug Des. Devel. Ther.* **2015**, *9*, 5851–5862.

[47] Jostes, S.; Nettersheim, D.; Fellermeyer, M.; Schneider, S.; Hafezi, F.; Honecker, F.; Schumacher, V.; Geyer, M.; Kristiansen, G.; Schorle, H. The Bromodomain Inhibitor JQ1 Triggers Growth Arrest and Apoptosis in Testicular Germ Cell Tumours *in Vitro* and *in Vivo*. *J. Cell. Mol. Med.* **2016**.

[48] Michaeloudes, C.; Mercado, N.; Clarke, C.; Bhavsar, P. K.; Adcock, I. M.; Barnes, P. J.; Chung, K. F. Bromodomain and Extraterminal Proteins Suppress NF-E2-Related Factor 2-Mediated Antioxidant Gene Expression. *J. Immunol. Baltim. Md 1950* **2014**.

[49] Floyd, S. R.; Pacold, M. E.; Huang, Q.; Clarke, S. M.; Lam, F. C.; Cannell, I. G.; Bryson, B. D.; Rameseder, J.; Lee, M. J.; Blake, E. J.; Fydrych, A.; Ho, R.; Greenberger, B. A.; Chen, G. C.; Maffa, A.; Del Rosario, A. M.; Root, D. E.; Carpenter, A. E.; Hahn, W. C.; Sabatini, D. M.; Chen, C. C.; White, F. M.; Bradner, J. E.; Yaffe, M. B. The Bromodomain Protein Brd4 Insulates Chromatin from DNA Damage Signaling. *Nature* **2013**, *498* (7453), 246–250.

[50] Choi, S.; Bakkenist, C. J. Brd4 Shields Chromatin from ATM Kinase Signaling Storms. *Sci. Signal.* **2013**, *6* (293), pe30.

[51] Lockwood, W. W.; Zejnullahu, K.; Bradner, J. E.; Varmus, H. Sensitivity of Human Lung Adenocarcinoma Cell Lines to Targeted Inhibition of BET Epigenetic Signaling Proteins. *Proc. Natl. Acad. Sci. U. S. A.* **2012**, *109* (47), 19408–19413.

[52] Ramos-Nino, M. E.; Timblin, C. R.; Mossman, B. T. Mesothelial Cell Transformation Requires Increased AP-1 Binding Activity and ERK-Dependent Fra-1 Expression. *Cancer Res.* **2002**, *62* (21), 6065–6069.

[53] Shaulian, E.; Karin, M. AP-1 in Cell Proliferation and Survival. *Oncogene* **2001**, *20* (19), 2390–2400.

[54] Bouchard, C.; Staller, P.; Eilers, M. Control of Cell Proliferation by Myc. *Trends Cell Biol.* **1998**, *8* (5), 202–206.

[55] Bretones, G.; Delgado, M. D.; León, J. Myc and Cell Cycle Control. *Biochim. Biophys. Acta* **2015**, *1849* (5), 506–516.

[56] Maritz, M. F.; van der Watt, P. J.; Holderness, N.; Birrer, M. J.; Leaner, V. D. Inhibition of AP-1 Suppresses Cervical Cancer Cell Proliferation and Is Associated with p21 Expression. *Biol. Chem.* **2011**, *392* (5), 439–448.

[57] Abbas, T.; Dutta, A. p21 in Cancer: Intricate Networks and Multiple Activities. *Nat. Rev. Cancer* 2009, 9 (6), 400–414.

[58] Galluzzi, L.; Vitale, I.; Michels, J.; Brenner, C.; Szabadkai, G.; Harel-Bellan, A.; Castedo, M.; Kroemer, G. Systems Biology of Cisplatin Resistance: Past, Present and Future. *Cell Death Dis.* **2014**, *5* (5), e1257.

[59] Gewirtz, D. A.; Holt, S. E.; Elmore, L. W. Accelerated Senescence: An Emerging Role in Tumor Cell Response to Chemotherapy and Radiation. *Biochem. Pharmacol.* **2008**, *76* (8), 947–957.

[60] Havelka, A. M.; Berndtsson, M.; Olofsson, M. H.; Shoshan, M. C.; Linder, S. Mechanisms of Action of DNA-Damaging Anticancer Drugs in Treatment of Carcinomas: Is Acute Apoptosis An "off-Target" effect? *Mini Rev. Med. Chem.* **2007**, *7* (10), 1035–1039.

[61] Delmore, J. E.; Issa, G. C.; Lemieux, M. E.; Rahl, P. B.; Shi, J.; Jacobs, H. M.; Kastritis, E.; Gilpatrick, T.; Paranal, R. M.; Qi, J.; Chesi, M.; Schinzel, A. C.; McKeown, M. R.; Heffernan, T. P.; Vakoc, C. R.; Bergsagel, P. L.; Ghobrial, I. M.; Richardson, P. G.; Young, R. A.; Hahn, W. C.; Anderson, K. C.; Kung, A. L.; Bradner, J. E.; Mitsiades, C. S. BET Bromodomain Inhibition as a Therapeutic Strategy to Target c-Myc. *Cell* **2011**, *146* (6), 904–917.

[62] Tolani, B.; Gopalakrishnan, R.; Punj, V.; Matta, H.; Chaudhary, P. M. Targeting Myc in KSHV-Associated Primary Effusion Lymphoma with BET Bromodomain Inhibitors. *Oncogene* **2013**.

[63] Venkataraman, S.; Alimova, I.; Balakrishnan, I.; Harris, P.; Birks, D. K.; Griesinger, A.; Amani, V.; Cristiano, B.; Remke, M.; Taylor, M. D.; Handler, M.; Foreman, N. K.; Vibhakar, R. Inhibition of BRD4 Attenuates Tumor Cell Self-Renewal and Suppresses Stem Cell Signaling in MYC Driven Medulloblastoma. *Oncotarget* **2014**, *5* (9), 2355–2371.

[64] Zhang, H.-T.; Gui, T.; Sang, Y.; Yang, J.; Li, Y.-H.; Liang, G.-H.; Li, T.; He, Q.-Y.; Zha, Z.-G. The BET Bromodomain Inhibitor JQ1 Suppresses Chondrosarcoma Cell Growth via Regulation of YAP/p21/C-Myc Signaling. *J. Cell. Biochem.* **2017**.

[65] Sekido, Y. Inactivation of Merlin in Malignant Mesothelioma Cells and the Hippo Signaling Cascade Dysregulation. *Pathol. Int.* **2011**, *61* (6), 331–344.

[66] Stocker, H. Growth Control: Myc and Yorkie Get Connected. *Curr. Biol. CB* **2011**, *21* (1), R37-39.

[67] Muramatsu, T.; Imoto, I.; Matsui, T.; Kozaki, K.-I.; Haruki, S.; Sudol, M.; Shimada, Y.; Tsuda, H.; Kawano, T.; Inazawa, J. YAP Is a Candidate Oncogene for Esophageal Squamous Cell Carcinoma. *Carcinogenesis* **2011**, *32* (3), 389–398.

[68] Dohi, T.; Xia, F.; Altieri, D. C. Compartmentalized Phosphorylation of IAP by Protein Kinase A Regulates Cytoprotection. *Mol. Cell* **2007**, *27* (1), 17–28.

[69] MANTEL, N. An Experimental Design in Combination Chemotherapy. *Ann. N. Y. Acad. Sci.* **1958**, *76* (3), 909-914-931.

[70] Ravera, M.; Gabano, E.; Bianco, S.; Ermondi, G.; Caron, G.; Vallaro, M.; Pelosi, G.; Zanellato, I.; Bonarrigo, I.; Cassino, C.; Osella, D. Host-Guest Inclusion Systems of Pt(IV)-Bis(benzoato) Anticancer Drug Candidates and Cyclodextrins. *Inorganica Chim. Acta*.

[71] Chou, T. C.; Talalay, P. Generalized Equations for the Analysis of Inhibitions of Michaelis-Menten and Higher-Order Kinetic Systems with Two or More Mutually Exclusive and Nonexclusive Inhibitors. *Eur. J. Biochem. FEBS* **1981**, *115* (1), 207–216.

[72] Singh, N. P.; McCoy, M. T.; Tice, R. R.; Schneider, E. L. A Simple Technique for Quantitation of Low Levels of DNA Damage in Individual Cells. *Exp. Cell Res.* **1988**, *175* (1), 184–191.

[73] Bright, J.; Aylott, M.; Bate, S.; Geys, H.; Jarvis, P.; Saul, J.; Vonk, R. Recommendations on the Statistical Analysis of the Comet Assay. *Pharm. Stat.* **2011**, *10* (6), 485–493.

[74] Singh, M.; Chaudhry, P.; Fabi, F.; Asselin, E. Cisplatin-Induced Caspase Activation Mediates PTEN Cleavage in Ovarian Cancer Cells: A Potential Mechanism of Chemoresistance. *BMC Cancer* **2013**, *13*, 233.

[75] Kuželová, K.; Grebeňová, D.; Brodská, B. Dose-Dependent Effects of the Caspase Inhibitor Q-VD-OPh on Different Apoptosis-Related Processes. *J. Cell. Biochem.* **2011**, *112* (11), 3334–3342.

[76] Dimri, G. P.; Lee, X.; Basile, G.; Acosta, M.; Scott, G.; Roskelley, C.; Medrano, E. E.; Linskens, M.; Rubelj, I.; Pereira-Smith, O. A Biomarker That Identifies Senescent Human Cells in Culture and in Aging Skin *in Vivo*. *Proc. Natl. Acad. Sci. U. S. A.* **1995**, *92* (20), 9363–9367.

[77] Friedrich, J.; Seidel, C.; Ebner, R.; Kunz-Schughart, L. A. Spheroid-Based Drug Screen: Considerations and Practical Approach. *Nat. Protoc.* **2009**, *4* (3), 309–324.

[78] Zanellato, I.; Bonarrigo, I.; Colangelo, D.; Gabano, E.; Ravera, M.; Alessio, M.; Osella, D. Biological Activity of a Series of Cisplatin-Based Aliphatic Bis(carboxylato) Pt(IV) Prodrugs: How Long the Organic Chain Should Be? *J. Inorg. Biochem.* **2014**, *140*, 219–227.

[79] Polovich, M.; Olsen, M.; LeFebvre, K. B. Chemotherapy and Biotherapy Guidelines and Recommendations for Practice (Fourth Edition) | ONS; Oncology Nursing Society, 2014.

[80] Matzuk, M. M.; McKeown, M. R.; Filippakopoulos, P.; Li, Q.; Ma, L.; Agno, J. E.; Lemieux, M. E.; Picaud, S.; Yu, R. N.; Qi, J.; Knapp, S.; Bradner, J. E. Small-Molecule Inhibition of BRDT for Male Contraception. *Cell* **2012**, *150* (4), 673–684.

[81] Cheng, Z.; Gong, Y.; Ma, Y.; Lu, K.; Lu, X.; Pierce, L. A.; Thompson, R. C.; Muller, S.; Knapp, S.; Wang, J. Inhibition of BET Bromodomain Targets Genetically Diverse Glioblastoma. *Clin. Cancer Res. Off. J. Am. Assoc. Cancer Res.* **2013**, *19* (7), 1748–1759.

[82] Zanellato, I.; Heldt, J.-M.; Vessières, A.; Jaouen, G.; Osella, D. Antiproliferative Effect of Ferrocifen Drug Candidates on Malignant Pleural Mesothelioma Cell Lines. *Inorganica Chim. Acta* **2009**, *362* (11), 4037–4042.

[83] Smith, M. L.; Chen, I. T.; Zhan, Q.; Bae, I.; Chen, C. Y.; Gilmer, T. M.; Kastan, M. B.; O'Connor, P. M.; Fornace, A. J. Interaction of the p53-Regulated Protein Gadd45 with Proliferating Cell Nuclear Antigen. *Science* **1994**, *266* (5189), 1376–1380.